Dust properties of galaxies at redshift z∼5-6

Ivana Barisic[1],
Supervisor: Dr. Peter L. Capak[2], and
Co-supervisor: Dr. Andreas Faisst[2]

[1]Physics Department, University of Zagreb, Zagreb, Croatia
[2]Infrared Processing and Analysis Center, California Institute of Technology, Pasadena, CA, USA

January 25, 2016

Abstract

Evolution of galaxies and their formation is still a project of study. Studying dust properties of galaxies at high redshift helps us to better understand properties of galaxies in general; what is their star formation rate, stellar population, metal content, etc. at earliest cosmic times. Therefore, it provides us with an insight into the evolution and formation of galaxies. In this project I am using new high resolution data measured by the *Hubble Space Telescope* Wide Field Camera 3 to study dust properties of Lyman-break galaxies observed in the COSMOS field, at a redshift between z∼5-6. My analysis shows bluer UV slope β values compared to the previous work (Capak et al. 2015). In this seminar I discuss the discrepancies with previous work, and methods used in data analysis.

1 Introduction

Lyman-break galaxies are normal galaxies observed at very high redshifts, characterized by, on average, higher star-formation rate compared to local galaxies. They are called Lyman-break since there is a discountinuity at the rest-frame wavelength of a galaxy at 912Å in their spectral energy distribution (SED). This wavelength is then called Lyman limit. They are important in investigating the formation and evolution of galaxies in the early universe, since unveiling their properties, such as stellar age, metal abundance, star formation rate, etc. helps us learn about properties of galaxies at early cosmic times [1]. The star-forming region of a Lyman-break galaxy is surrounded with neutral hydrogen gas. Photons of wavelengths longer than the Lyman limit emitted from the star-forming region are not energetic enough to ionize the neutral gas so they pass through the gas and observer can detect these emission lines. However, photons of wavelengths of 912Å and below the limit are energetic enough to ionize the neutral gas and galaxy appears very dim at those wavelengths, since rare photons at 912 Å wavelength and below can pass through the region of neutral gas without ionizing it. These galaxies are very far away, so due to the expansion of the universe wavelengths that pass through the neutral gas region will be shifted towards longer wavelengths, i.e. will be redshifted. The longer the distance between the source and the observer, the bigger the shift to longer wavelengths. Figure 1 shows a model SED fit for a galaxy at redshift $z = 5.8$. On the x-axis is the rest frame wavelength and on the y-axis is the normalized flux. In the case galaxy contains no dust, its SED is represented by a solid black curve. However, if galaxy is dust-rich, the ultraviolet emission from the star-forming region will heat up the dust and this radiation will be reemitted in the infrared part of the electromagnetic spectrum. The SED of a dust-rich galaxy is represented with a dashed black curve. The steepness of the slope of the line is an indicator of the amount of dust in the line of sight of an observer. A flatter slope indicates more dust-rich system. Therefore, blue line with

[1]`http://pendientedemigracion.ucm.es/info/Astrof/users/jgm/GiavaliscoARAA.pdf`

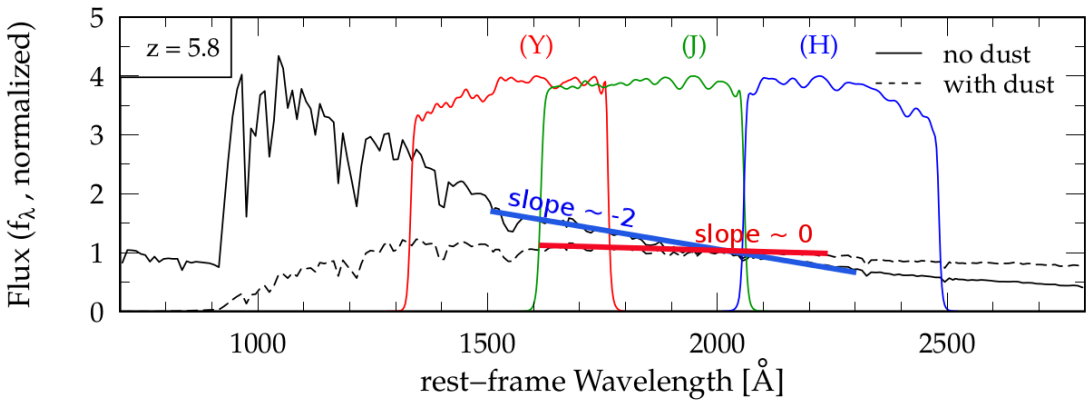

Figure 1: The model Spectral Energy Distribution (SED) fit for a galaxy at a redshift 5.8. Solid curve represents the SED of a galaxy with no dust content. The SED of a dust-rich galaxy is represented with a dashed curve. The slope of fitted lines (blue and red) indicate the amount of dust along the line-of-sight of an observer. The steeper the slope is, less dust obscured system is in the line-of-sight of an observer.

a steepness of the slope ∼-2 represents a dust-poor system, while red line of a slope steepness ∼0 represents a dust-rich system. The steepness of the slope is usually called ultraviolet (UV) slope β which I will refer to at a later point.

2 Data

The sample consists of 9 Lyman-break galaxies and a quasar at redshifts z∼5-6 observed in the Cosmological Evolution Survey (COSMOS) field. The COSMOS is a 2 square degree survey for studying properties of galaxies as a function of redshift [2]. The measurements were done by the *Hubble Space Telescope* Wide Field Camera 3 (HST WFC-3), and are very deep and high resolution (up to z≃7 - 9; 1 pixel in the image corresponds to 0.13"). The measurements were taken in three different filters at 1μm (Y band), 1.25μm (J band), and 1.65μm (H band). These wavelengths correspond to the near infrared (NIR) part of the electromagnetic spectrum. Taking into account the redshift of the objects in the sample, we are probing the UV emission in the rest-frame of objects in the sample. This dataset enables me to accurately compute the UV slope β for each object in the sample, which is an indicator of dust content. Galaxies in the sample with associated redshifts are shown in Figure 2. I also used the HST WFC-3 data to obtain UV luminosities of objects in the sample. The measurement in the rest-frame far infrared (FIR) was done using early (20 antenna; resolution 0.6"/pixel) version of the Atacama Large Millimeter Array (ALMA), and this data point is used to estimate IR luminosities (for more details refer to Capak et al. 2015). The sensitive and high resolution (final 66 antenna version will be up to 50 milliarcsec/pixel [3]) ALMA measurements are of great importance for investigating the dust properties of galaxies, due to its abillity to probe the rest-frame IR emission of high redshift galaxies [4]. Both of these instruments are worlds top instruments for probing galaxies at high redshift, therefore making us able to accurately investigate the formation and evolution of galaxies.

3 Method

To extract the photometry of the sources I used the software *Source Extractor* (Bertin & Arnouts 1996). Sources of interest in images are very faint

[2] http://cosmos.astro.caltech.edu/
[3] http://www.almaobservatory.org/en/about-alma/how-does-alma-work/technology/interferometry
[4] http://www.almaobservatory.org/en/about-alma

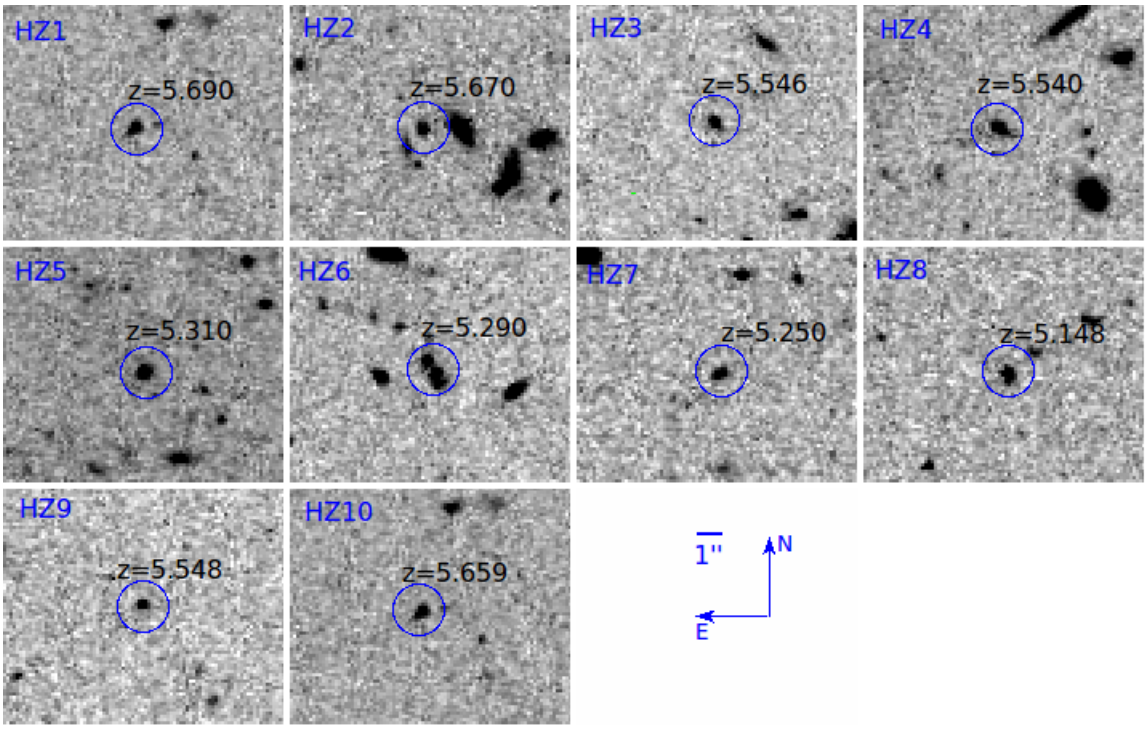

Figure 2: Images of the sources from the sample taken by the *Hubble Space Telescope* Wide Field Camera 3. Selected regions are 2.05" in radius.

(order of magnitude $\sim 10^{-19}$[erg/s/cm^2/Å]), so it is important to set a threshold to cut-off the background noise, while conserving the source. The chosen threshold is 2σ. When extracting the photometry one needs to choose the aperture sizes for sources in images. The *Source Extractor* offers ISO, AUTO and manual apertures which sizes are arbitrary. The ISO aperture is isophotal, meaning it is set by following the pixels of the constant brightness in the image. The AUTO aperture is ellipticaly shaped and is flexible so it fits the size of an object. Manual apertures were picked by optically examining the images in the program *SAOImage DS9* in a way that a chosen aperture size includes the galaxy, and is not being contaminated by the surrounding sources. The chosen apertures have radii of 1.54", 1.80", 2.05". Manual aperture sizes are the same in all images for all sources. After running the *Source Extractor* one obtains a catalog with the photometric data of all of the sources for each filter. The sources are then cross-matched in each band to obtain final fluxes in the near-IR, after which UV slopes β are measured in a way:

$$f_\lambda = \lambda_{rest}^{\beta} \tag{1}$$

The logarithm of the relation above gives

$$log f_\lambda = \beta \cdot log \lambda_{rest} + const. \tag{2}$$

where f_λ represents the flux density in [erg/s/cm^2 / Å], and λ_{rest} represents the rest-frame wavelength of the observed galaxy in [Å]. The dependence of logarithm of the flux versus the rest-frame wavelength λ is shown in Figure 3. The vertical line represents the UV 1600Å line.

3.1 Monte Carlo iterations for flux density uncertainity

Running Monte Carlo iterations enabled me to determine the uncertainities in the UV slopes β. The number of iterations was set to 1000. Known flux density values in each band were used as mean values for randomly generating output flux densities from of a Gaussian distribution. Varied output fluxes from different bands were then used to compute UV slope β. The mean value of newly generated UV slope β values agreed with the input

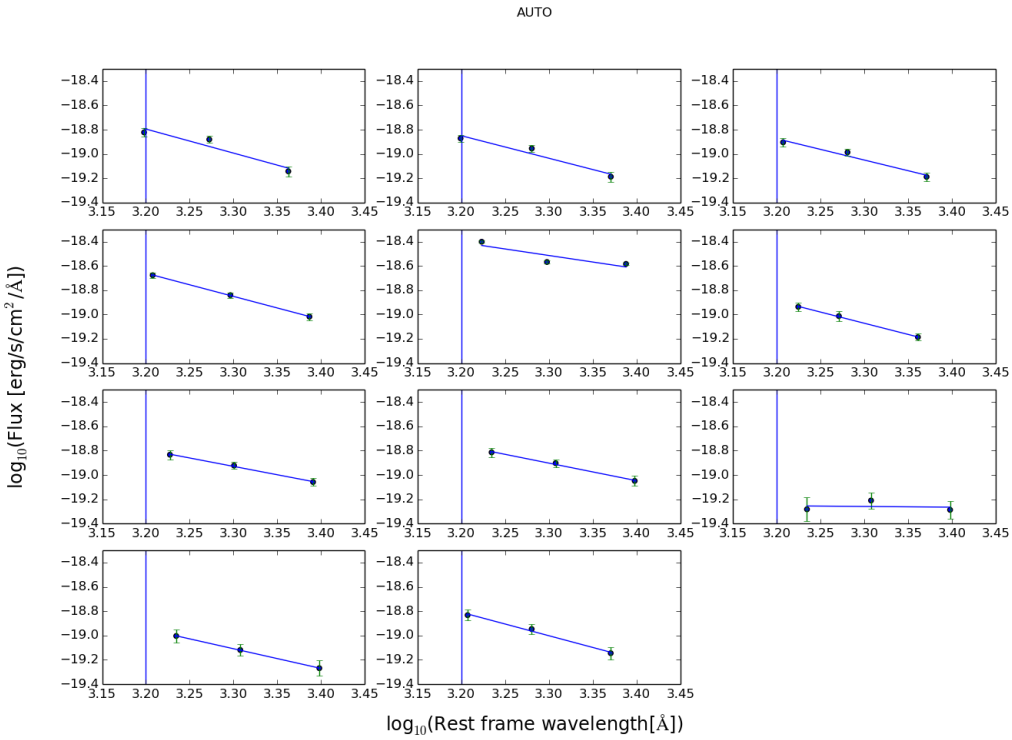

Figure 3: Logarithm of the flux density vs rest-frame wavelength λ_{rest}. There are 9 galaxies and a quasar, however HST WFC-3 data shows a possible companion for one of the sources, so Figure 3 contains 11 panels. Fitted slope in each of the panels represents the UV slope β which is an indicator of dust obscuration in galaxies in the line of sight of an observer. Vertical line represents the 1600 Å line.

UV slope β value. The error bars on flux densities were found as 1σ of the Gaussian distribution of random output flux densities.

3.2 Monte Carlo simulations to find systematic effects

To study the systematic effects I was running Monte Carlo simulations. I created mock galaxies and insterted them to original images. Mock galaxies are parametrized by the 2D Gaussian and then added to the original images taken by the HST WFC-3. I randomly generated 10 flux densities in a range $[10^{-20}, 10^{-18}]$[erg/s/cm^2/Å], 10000 UV slope β values in a range [-5,2], and 100 coordinates. The *Source Extractor* generates the segmentation map of the original image in which empty pixels represent areas with no detections. After stacking original segmentation maps of a single source in all three bands into one segmentation map, mock galaxies were inserted in areas of original images that correspond to empty pixels in the stacked segmentation map. I ran the *Source Extractor* to extract the photometry and obtain photometric catalogs of the newly generated image. Next step was cross-matching the known randomly generated coordinates with the coordinates from catalogs to get the photometry of mock galaxies. Therefore, in the case of very faint flux densities ($\sim 10^{-20}$[erg/s/cm^2/Å]) it can occur that mock galaxy is detected by the *Source Extractor* only in one or two bands, rarely in all three bands. It is not possible to compute the UV slope β if the flux was detected only in one band. If the flux is detected in two bands the UV slope β can be computed, however, β values obtained this way are less precise.

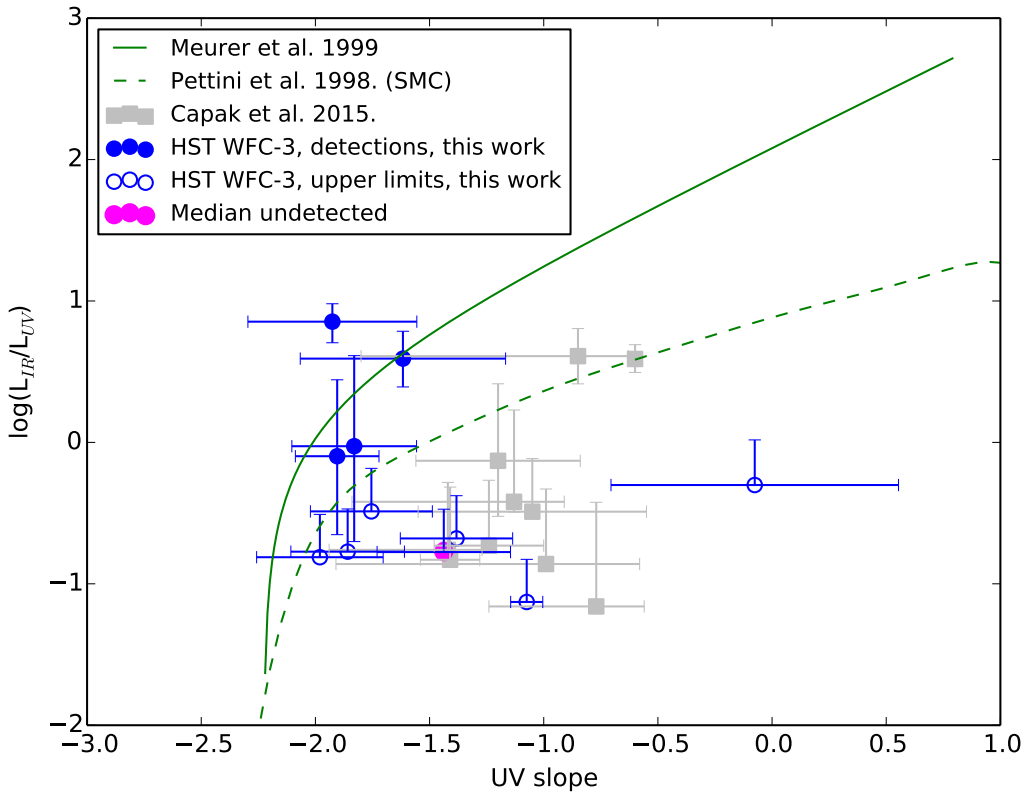

Figure 4: The ratio of infrared to ultraviolet luminosity (L_{IR}/L_{UV}) as a function of the UV slope β. Blue filled circles represent detections by the HST WFC-3 and the ALMA, while blue empty circles are upper limits detected only by the HST WFC-3. Green solid curve represents the local metal rich and dust obscured starburst galaxies. Green dashed curve represents the SMC curve which is a representative of the dust and metal poor system. Gray squares represent the results of the previous work (Capak et al. 2015)

4 Results

The UV slope β in general represents the dust abundance of the source in the observers line-of-sight. Figure 4 shows the dependence of the logarithm of the luminosity ratio (L_{IR}/L_{UV}) versus UV slope β. The luminosity ratio represents the total amount of dust in the galaxy. The higher the ratio of infrared to ultraviolet luminosity, the higher the dust obscuration in the galaxy. IR luminosities L_{IR} were estimated by the ALMA (Capak et al. 2015), while UV luminosities L_{UV} are obtained by the HST WFC-3 measurements. Both, blue filled and empty circles represent the detections of this work. Blue filled circles represent the detections by the HST WFC-3 and the ALMA, while blue empty circles represent the upper limits. Green solid curve represents the local starburst galaxies, which are metal-rich and dust-rich systems (Meurer et al. 1999). Green dashed curve represents the curve of the Small Magellanic Cloud (SMC, Rodrigues et al. 1997) like system, which is the system low in dust content, metal poor and young. Grey squares show results of the previous work by Capak et al. 2015. It is evident that the UV luminosity values observed by the HST WFC-3 are lower, resulting in the higher ratio of IR to UV luminosity. There is a significant discrepancy between UV slope β values obtained from the HST WFC-3 data ($\langle\beta\rangle \sim$ -1.5) and pre-

vious work ($\langle\beta\rangle \sim$ -1.0, Capak et al. 2015) which used the ground based telescope data to estimate UV slope β values. I obtained bluer UV slope β values, which means that galaxies in the sample are less dust-rich from what previous work shows. This result is closer in agreement with other works that analyzed space based data, where they find that galaxies at redshift z=6-7 have the mean UV slope $\langle\beta\rangle \leq$ -2.5 (Bouwens et al. 2012) From the Figure 4 it is evident that detections might fall into two distinct populations. The continuum detections (blue filled circles) agree with the Meurer et al. 1999 curve, meaning that properties of these galaxies agree with the local dust-rich and high metalicity starburst galaxies. The upper limit detections (blue empty circles) agree with the SMC like curve which represents local dust-poor and metal poor young systems. Taking into account that those are only upper limits detections, further observations are required. Even though HST WFC-3 data are much deeper and more accurate, further investigation is required in order to find out about systematic effects in measurements. We expect lower systematic biases in measurements compared to previous work, due to the high signal-to-noise ratio od the HST WFC-3 measurements.

After running Monte Carlo simulations (described in 3.2) I compared the output UV slope β values to the input ones and plotted their difference as a function of the logarithm of the input flux density at 1600Å , which is shown in Figure 5. The expected value of the difference between input and retrieved UV slope β values is ideally 0. In Figure 5 detections from simulations are represented by light blue circles, while median values are represented by yellow circles. Error bars on the y-axis are computed as the 68 percentile of the (β_{out}-β_{in}) distribution for a certain flux density value.

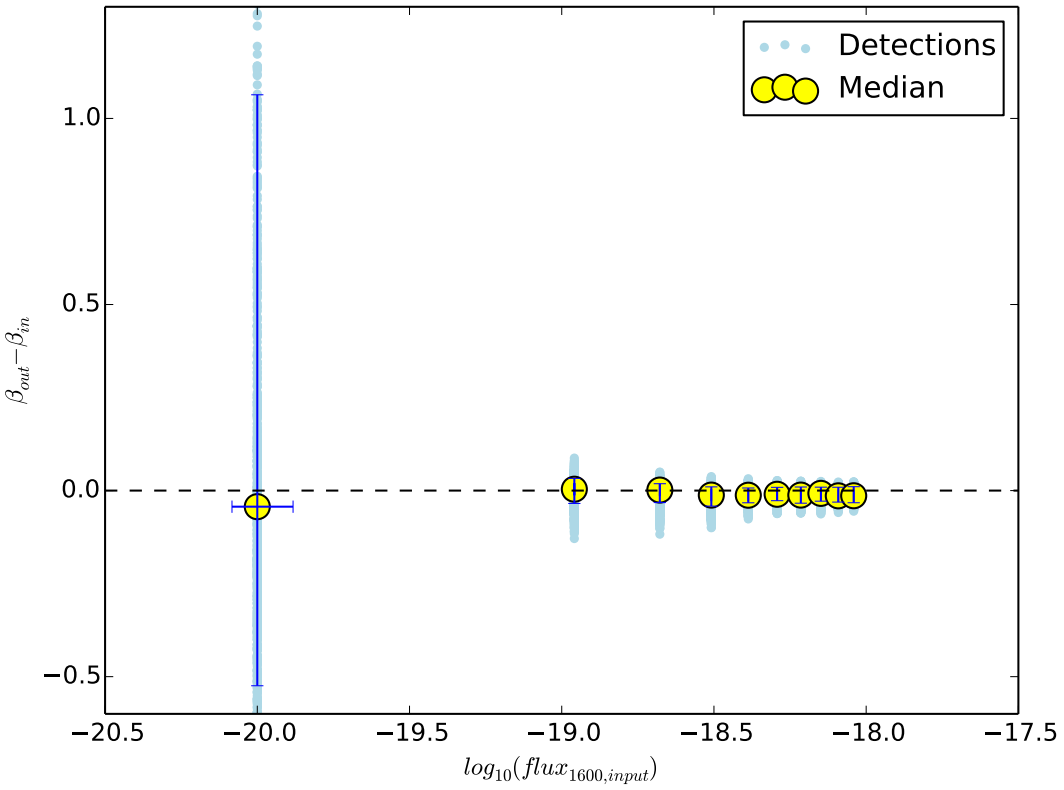

Figure 5: The difference between retrieved UV slope value from simulations and the input UV slope (β_{out}-β_{in}) as a function of the logarithm of the input flux density at 1600Å

Error bars on the x-axis are found as the 68 percentile of the ($\log_{10}(f_{1600,output})$-$\log_{10}(f_{1600,input})$) distribution. We can see from the y-axis error bars that the offset from the expected value is less than 10%, except in the faintest flux case, $\log(flux_{1600,input})$=-20 where the detections have a large scatter. The reason for such large scatter is in computing β values from only two flux density detections, which is less precise, then in the case when all three flux density values are available. We can say that sources with such flux density values are too faint and hardly distinguishable from the background noise. Overall, differences between retrieved and input β values are consistent with the expected value, meaning that the computed β values for galaxies in the original image are not much altered by the software extracting the photometry. The plot of difference between input and output β value as a function of the output AB magnitudes at 1600Å is shown in Figure 6, where on the top of each panel is the input AB magnitude at 1600Å. Each panel shows the scatter of recovered magnitude values compared to the input magnitude value. The x-axis has been divided into 5 intervals in a way that each interval has the equal number of points. Then median values (yellow circles) were found in each interval, and error bars on the y and x-axis are found respectively as the 68 percentile of the distribution of difference in β and difference in AB magnitudes. It is evident that if the *Source Extractor* extracts higher flux density values at 1600Å(corresponds to higher magnitudes), the recovered β is more negative than the input one, resulting in negative difference between output and input UV slope β values, which is the behaviour we see in each panel. Furthermore, detections at higher output AB magnitudes in each panel are inconsistent with the expected value (zero). However, further tests are required and this is still an ongoing process.

5 Summary and Conclusions

In this work I used the high signal-to-noise and high resolution HST WFC-3 data to investigate dust properties of galaxies at redshift between z∼5-6. From the HST WFC-3 data I computed the UV slope β values and determined the UV luminosities of sources from the sample. For IR luminosities I used the estimated values obtained by the ALMA measurements from Capak et al. 2015. The results I obtained, shown in Figure 4, possibly indicate that sample consists of two different populations. One of which are detections by both HST WFC-3 and the ALMA and which agree with the Meurer et al. 1999 like curve, being a representative of a local starburst metal rich and dust-rich systems, and upper limits which coincide with the SMC like curve, a representative of a local dust-poor and metal poor system. This further suggests that some of the systems in the sample are young, in the process of formation, while others have already formed and are therefore chemically enriched. However, this is going to be under a further investigation to find out more about the sources from the sample. Simulations (see Figure 5) show there are no systematic effects in recovered β values and that the difference in β are consistent with the expected value. This further indicates that software used to extract photometry does not significantly affect measurements. However, further tests on systematic effects are being conducted.

Acknowledgements

I would like to thank my supervisors, Dr. P. Capak and Dr. A. Faisst for guiding me throughout the project, as well as to Micaela Bagley and Assoc. Prof. V. Smolcic for helpful discussions.

References

Capak, P. L., Carilli, C., Jones, G., et al. 2015, Nature, 522, 455

Meurer, G. R., Heckman, T. M., & Calzetti, D. 1999, The Astrophysical Journal, 521, 64

Bertin, E., & Arnouts, S. 1996, American Astronomical Society, 117, 393

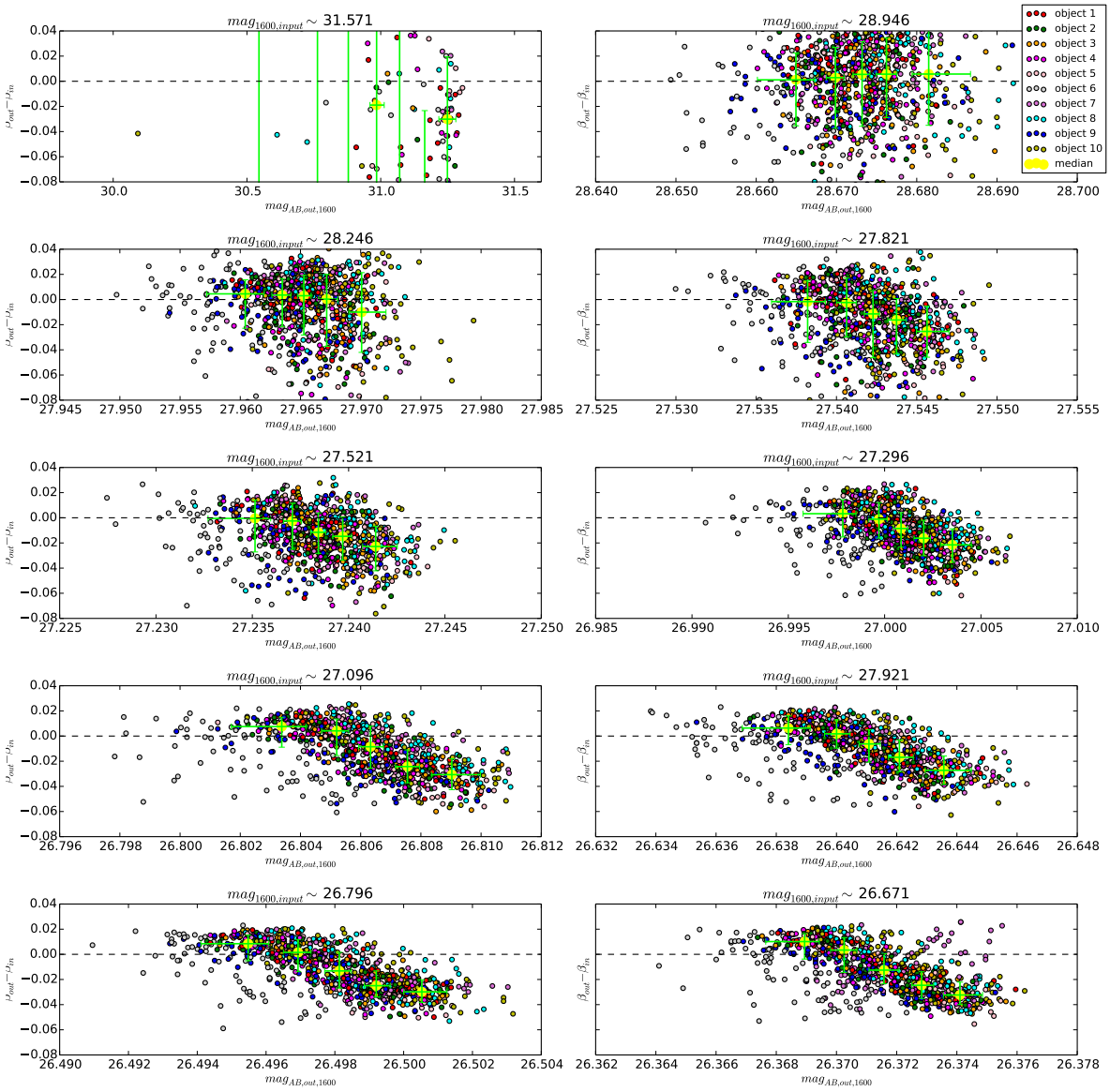

Figure 6: The difference between retrieved and input UV slope (β_{out}-β_{in}) as a function of output AB magnitude. Panels represent each of the input magnitude values at 1600Å.

Rodrigues, C. V., Magalhães, A. M., Coyne, G. V., & Piirola, S. J. V. 1997, The Astrophysical Journal, 485, 618

MacKenty, J. W., Baggett, S. M., Brammer, G., et al. 2014, Proceedings of the International Society for Optical Engineering, 9143, 914328

Bouwens, R. J., Illingworth, G. D., Oesch, P. A, et al. 2012, The Astrophysical Journal